

Research Article

Selective Inhibition of NMDA receptors with GluN2B subunit protects beta cells against stress-induced apoptotic cell death

Anne Gresch^{a§}, Héctor Noguera Hurtado^{a§}, Laura Wörmeyer^a, Vivien De Luca^a, Rebekka Wiggers^a, Guiscard Seebohm^b, Bernhard Wunsch^c, Martina Düfer^a

^a Pharmaceutical and Medicinal Chemistry, Dept. of Pharmacology, PharmaCampus, University of Münster, Corrensstraße 48, 48149 Münster, Germany

^b Institute for Genetics of Heart Diseases (IfGH), Department of Cardiovascular Medicine, University Hospital Münster, D-48149 Münster, Germany.

^c Pharmaceutical and Medicinal Chemistry, PharmaCampus, University of Münster, Corrensstraße 48, 48149 Münster, Germany

[§]A. Gresch and H. Noguera Hurtado contributed equally to this work.

Running title: NMDA receptor inhibition protects pancreatic beta cells

Section assignment for table of contents: Endocrine and Diabetes

Corresponding Author:

Prof. Dr. Martina Düfer

Pharmaceutical and Medicinal Chemistry, Dept. of Pharmacology,

PharmaCampus, University of Münster

Corrensstraße 48, 48149 Münster, Germany

Phone: 49 251 83 33339; Fax: 49 251 83 32144

martina.duefer@uni-muenster.de

Text pages: 18

Tables: 0

Figures: 6

References: 36

Word count:

Abstract: 250

Introduction: 465

Discussion: 1579

Keywords: apoptosis, beta cell, GluN2B, NMDA receptor, insulin secretion

Abbreviations: a.u.: arbitrary fluorescence units, CNS: central nervous system, FOPP: fraction of plateau phase, K_{ATP} channel: ATP-dependent K^+ channel, MEA: microelectrode array, NMDA(R): N-methyl-D-aspartate (receptor), Ro 25-6981: ($\alpha R, \beta S$)- α -(4-hydroxyphenyl)- β -methyl-4-(phenylmethyl)-1-piperidine propanol, V_m : membrane potential, WMS-1410: 3-(4-phenylbutyl)-2,3,4,5-tetrahydro-1*H*-3-benzazepine-1,7-diol.

Abstract

Participation of NMDA receptors (NMDARs) in the failure of pancreatic beta cells during development of type 2 diabetes mellitus is discussed. Our study investigates whether beta cell mass and function can be preserved by selectively addressing the GluN2B subunit of the NMDAR. NMDAR activation by NMDA and its co-agonist glycine moderately influenced electrical activity and Ca^{2+} handling in islet cells at a threshold glucose concentration (4-5 mM) without affecting glucose-mediated insulin secretion. Exposure of islet cells to NMDA/glycine or a glucolipotoxic milieu increased apoptosis by 5 and 8 %, respectively. The GluN2B-specific NMDAR antagonist WMS-1410 (0.1 and 1 μM) partly protected against this. In addition, WMS-1410 completely prevented the decrease in insulin secretion of about 32 % provoked by a 24-h-treatment with NMDA/glycine. WMS-1410 eliminated NMDA-induced changes in the oxidation status of the islet cells and elevated the sensitivity of intracellular calcium to 15 mM glucose. By contrast, WMS-1410 did not prevent the decline in glucose-stimulated insulin secretion occurring after glucolipotoxic culture. This lack of effect was due to a decrease in insulin content to 18 % that obviously could not be compensated by the preservation of cell mass or the higher percentage of insulin release in relation to insulin content. In conclusion, the negative effects of permanent NMDAR activation were effectively counteracted by WMS-1410 as well as the apoptotic cell death induced by high glucose and lipid concentrations. Modulation of NMDARs containing the GluN2B subunit is suggested to preserve beta cell mass during development of type 2 diabetes mellitus.

Significance statement

Addressing NMDA receptors containing the GluN2B subunit in pancreatic islet cells has the potential to protect the beta cell mass that progressively declines during the development of type 2 diabetes. Furthermore, this study shows that harmful effects of permanent NMDAR activation can be effectively counteracted by the compound WMS-1410, a selective modulator for NMDARs containing the GluN2B subunit.

Introduction

The glutamate-gated N-methyl-D-aspartate receptor (NMDAR) plays a central role in the mammalian central nervous system (CNS). Amongst others, it participates in neuronal development, synaptic plasticity, learning, and memory formation. Functional NMDARs are heterotetrameric ion channels containing two obligatory GluN1 subunits combined with GluN2 and / or GluN3 subunits. At least 8 splice variants are known for the GluN1 subunit, that can associate with different isoforms of GluN2 (A-D) or GluN3 (A or B). The GluN2 subunit plays a very important role for channel characteristics, with important differences among the isoforms, e.g. regarding channel decay rate and thus the time for Ca^{2+} influx (Paoletti et al., 2013; Zhang & Luo, 2013). Apart from their physiological function in development and learning, NMDARs are known mediators of neuronal damage when activated in excess or permanently. GluN2B is thought to be a “bad guy” under conditions fostering excitotoxicity (Mony et al., 2009). Consequently, reducing NMDAR activity by targeting NMDARs with GluN2B subunit is the focus of research for treatment of a variety of neuroinflammatory or neurodegenerative CNS disorders, including chronic pain, stroke, Alzheimer’s or Parkinson’s disease (Chazot, 2004). One of the first compounds shown to inhibit GluN2B with high affinity was ifenprodil (Williams, 1993). To improve specificity and to reduce side effects, antagonists with tetrahydro-3-benzazepine-1,7-diol scaffold have been designed by exchanging the piperidine ring of the lead compound to a benzazepine. (Tewes et al., 2010a). The compound WMS-1410 (3-(4-phenylbutyl)-2,3,4,5-tetrahydro-1*H*-3-benzazepine-1,7-diol) (Fig. 6A, (a)) represents the most promising GluN2B antagonist of this series. WMS-1410 is characterized by a high selectivity, an increased half-life compared to ifenprodil and good *in vivo* tolerability (Tewes et al., 2010a). Since neurons and β -cells share characteristic features, e.g. the close coupling of exocytosis of secretory granules to electrical activity (Arntfield & van der Kooy, 2011), it is not surprising that NMDARs are expressed in pancreatic islets. GluN1 and GluN2 subunits were detected on the level of mRNA and protein in insulin-secreting cell lines and rodent islets (Gonoi et al., 1994; Inagaki

et al., 1995; Atouf et al., 1997; Morley et al., 2000). The NMDAR is assigned a physiological role within a negative feedback loop controlling pulsatile insulin secretion (Takahashi et al., 2019) as well as a pathophysiological impact during chronic stimulation by high glucose concentrations (Huang et al., 2017a). Up to now, nothing is known about subtype-specific modulation of the NMDAR and its significance for beta cell regulation.

The aim of our study was to elucidate whether inhibition of NMDAR via the GluN2B subunit is suited to interfere with beta cell signaling and viability under conditions of increased substrate supply. To address this issue Ca^{2+} signaling, electrical activity, insulin release, oxidative status, and apoptotic cell death were determined in mouse islets or islet cells and the 3-benzazepine derivative WMS-1410 was used for selective targeting of GluN2B.

Materials and Methods

Cell and islet preparation

Experiments were conducted with islets of Langerhans or single islet cells from adult male and female C57BL/6N mice (Charles River, Sulzfeld, Germany and own breeding, Institute of Pharmaceutical and Medicinal Chemistry, Münster, Germany). The principles of laboratory animal care were followed according to German laws (Az. 53.5.32.7.1/MS-12668, health and veterinary office Münster, Germany). Mice were euthanized using CO_2 and pancreatic islets were isolated by collagenase digestion. Islets were dispersed to single cells by trypsin treatment. Islets or cells were cultured in RPMI 1640 medium (11.1 mM glucose) supplemented with 10 % fetal calf serum, 100 U/ml penicillin, and 100 μ g/ml streptomycin at 37°C in 5 % CO_2 humidified atmosphere. After preparation, islets or dispersed islet cells were kept overnight in standard culture medium. Next day, medium was replaced by either standard medium \pm indicated substances or by glucolipotoxic medium (RPMI medium with 33 mM glucose combined with 10 μ M T0901317 or 500 μ M sodium palmitate, 0.28 % fatty

acid free BSA) in the presence or absence of WMS-1410, Ro 25-6981 or memantine for the specified time periods.

Solutions and chemicals

Krebs-Ringer-HEPES solution (KRH) for insulin secretion was composed of (in mM): 122 NaCl, 4.7 KCl, 1.1 MgCl₂, 2.5 CaCl₂, 10 HEPES, glucose as indicated, 0.5 % bovine serum albumin (BSA) and pH 7.4 adjusted with NaOH. Electrophysiological measurements, recordings of [Ca²⁺]_c and redox status were performed with a bath solution of (in mM): 140 NaCl, 5 KCl, 1.2 MgCl₂, 2.5 CaCl₂, 10 HEPES, glucose as indicated, pH 7.4 adjusted with NaOH. Pipette solution for recording the plasma membrane potential (V_m) consisted of (in mM): 10 KCl, 10 NaCl, 70 K₂SO₄, 4 MgCl₂, 2 CaCl₂, 10 EGTA, 5 HEPES, 0.27 amphotericin B, pH adjusted to 7.15 with KOH. The palmitate-containing medium was prepared as described previously (Schultheis et al., 2019). In experiments with NMDA, if islet cells or islets were treated with KRH or bath solution the NMDAR co-activator glycine (10 μM) was added together with NMDA. The RPMI 1640 culture medium already contains 0.13 mM glycine.

Collagenase P was ordered from Roche Diagnostics (Mannheim, Germany), Corning[®] Matrigel[®] basement membrane preparation from VWR (Darmstadt, Germany), RPMI 1640, fetal calf serum and penicillin/streptomycin from Life Technologies (Darmstadt, Germany). Fura-2 acetoxymethylester (fura-2 AM) and rat insulin were ordered from Biotrend (Köln, Germany). N-methyl-D-aspartic acid (NMDA), Ro 25-6981, glutamate and glycine were from Sigma-Aldrich (Taufkirchen, Germany), memantine from Fisher Scientific (Schwerte, Germany) and T0901317 was from Biomol (Hamburg, Germany). All other chemicals were from Sigma-Aldrich (Taufkirchen, Germany) or Diagonal (Münster, Germany). WMS-1410 was synthesized at the Institute of Pharmaceutical and Medicinal Chemistry (Münster, Germany) as described in Tewes et al., 2010b.

Insulin secretion

After preparation, islets were kept overnight in RPMI medium. Next day, the culture medium was exchanged for the medium \pm substances in case of a pre-treatment. At the day of the assay, islets were incubated in KRH with 5.6 mM glucose for 1 hour and thereafter in KRH buffer with 3 mM glucose for 0.5 hours to reduce insulin secretion to a basal level. Test compounds were no longer present in case of a pre-treatment during the silencing period except for the 24 h-pre-incubation experiment. For determination of insulin secretion, 15 islets for each condition were incubated in batches of five islets at 37°C for 1 hour with the indicated glucose concentrations and substances (only in experiments with acute exposure to the test compounds). Insulin concentration was quantified by a radioimmunoassay using rat insulin as standard.

Measurement of redox status and $[Ca^{2+}]_c$

Islets or dispersed islet cells were cultured for 1-2 days on glass coverslips. For islets, glass coverslips were coated with poly-L-lysine. Islets or isolated cells were loaded in bath solution with fura-2 AM (5 μ M, 15 mM glucose \pm indicated substances, 37°C, 30 minutes) or 2', 7'-dichlorodihydrofluorescein-diacetate (DCDHF-DA, 20 μ M, 10 mM glucose, 37°C, 15 minutes) and thereafter maintained in bath solution. For determination of DCF fluorescence and $[Ca^{2+}]_c$ after pre-incubation, the test compounds were omitted from the bath solution during the recordings. Fluorescence was excited at 340 nm and 380 nm every 3 seconds ($[Ca^{2+}]_c$) or at 480 nm for 3 consecutive images in 50 millisecond intervals (DCF) and emission was measured by a digital camera (filter 515 nm). Alterations in mean Ca^{2+} were evaluated by calculating the average of the mean Ca^{2+} concentration in bath solution with 15 mM glucose for 15 minutes before glucose concentration was changed. To confirm that the islets or islet cells were metabolically intact bath solution with 0.5 or 15 mM glucose was applied at the beginning or at the end of each experiment. Pancreatic beta cells exhibit characteristic

glucose-evoked oscillations, which disappear in the presence of a low glucose concentration (Grapengiesser et al., 1988). For determination of DCF fluorescence two culture dishes were prepared for each condition per mouse preparation. DCF fluorescence was analysed in two randomly chosen areas of each culture dish by averaging three consecutive measurements per cell. All cells per dish were averaged and one data point represents the mean of the two samples per mouse preparation.

Electrophysiology

Patch-clamp experiments were performed with single islet cells. An EPC-10 patch-clamp amplifier (HEKA, Germany, software “Patchmaster” and “Fitmaster”) was used for data acquisition and analysis. Pipettes were pulled from borosilicate glass capillaries (resistance of 3-5 M Ω). V_m was measured in the current clamp mode and evaluated by determination of the membrane potential for a period of 1 minute before changing bath solution. Cells were identified as β -cells by glucose-dependent appearance of action potentials. Electrical activity of whole islets was determined by extracellular membrane potential recordings with microelectrode arrays (MEA2100-system with 60MEA200/30iR-Ti-gr, Multi Channel Systems, Reutlingen, Germany). Islets were cultured for 3 to 4 days on microelectrode arrays (MEAs) coated with Matrigel[®]. Medium was changed to bath solution with 3 mM glucose at the beginning of each experiment. Thereafter, glucose was elevated to 8 mM, followed by addition of test compounds as indicated. Data were low-pass filtered at 25 Hz and sampled at 1000 Hz (MC-Rack software). For analysis, the fraction of plateau phase (FOPP, i.e. time with bursting activity related to the entire time interval) was calculated at the end of each experimental maneuver for a period of 20 min.

Apoptosis assay

For determination of the percentage of apoptotic cells a TUNEL assay (in situ cell death detection kit, fluorescein, Roche Diagnostics) was used. After the specified incubation time,

islets cells were washed with phosphate-buffered saline, fixed with paraformaldehyde 3% and permeabilized (0.1 % Triton-X on ice, 2 minutes). The samples were stained with TUNEL reaction mixture for 1 hour, followed by a nuclear staining with Hoechst-33258 for 10 minutes at room temperature in the absence of light. After nuclei staining, samples were excited at 380 nm and fluorescence of apoptotic cells was detected at 480 nm. Apoptosis was determined by counting the number of TUNEL-positive cells in relation to all cells in 10 randomly selected fields of each sample (300-400 cells for each mouse islet cell preparation).

Statistics

Data were collected from islets or islet cells of at least three independent mouse preparations for each series of experiments. Values are given as scatter plots and means \pm SD. Data were normally distributed (GraphPad Prism 3.00). The null hypothesis of each series of experiments was that the test compound has no influence on the respective parameter. Statistical significance was assessed by paired (Fig. 3) or unpaired (Suppl. Fig. 1B) Student's t-test, or by ANOVA followed by Student-Newman-Keuls post hoc test for multiple comparisons (Fig. 1, 2, 4 and 5, Suppl. Fig. 1A). GraphPad Prism Windows version 3.00 (GraphPad Software) was used for analysis. Values of $p \leq 0.05$ were considered as statistically significant.

Results

Inhibition of NMDARs containing the GluN2B subunit interferes with the redox status of murine islet cells and protects against NMDA-induced cell damage

Constant activation of NMDAR is linked to cell death and oxidative stress. At first, it was tested whether subtype-specific inhibition of activated NMDAR interferes with the general oxidation status of islet cells. To address this question the ROS-sensitive dye DCDHF was used and its oxidation to DCF was monitored. Culturing islet cells in standard medium, containing the NMDAR co-activator glycine and supplemented with 5 mM NMDA (Huang et al., 2017b) for 48 hours increased the fluorescence of DCF. WMS-1410 had no influence on DCF fluorescence *per se* but completely prevented the effect of NMDA (Fig. 1A). As these results suggest that targeting the GluN2B subunit of NMDAR makes the islet cells more resistant to oxidative stress, we elucidated, whether inhibition of NMDAR by WMS-1410 can protect against apoptosis. Isolated islet cells were treated with NMDA at a concentration of 500 μ M, combined with 10 μ M glycine, in the presence or absence of WMS-1410 for 18 hours. Prolonged activation of NMDAR resulted in a marked increase in apoptotic islet cells (Fig. 1B and C, grey vs. white bars). WMS-1410 clearly reduced this effect when applied at concentrations of 1 μ M (Fig. 1B) or 0.1 μ M (Fig. 1C) in parallel with NMDA. To see, whether the NMDA-induced reduction of islet cell mass affects insulin release, insulin secretion was determined after 24-h culture of whole islets with or without NMDA (500 μ M) in standard medium containing glycine. Permanent activation of NMDAR decreased insulin release in response to 15 mM glucose (1 hour) by ~30 % (Fig. 1D). Importantly, co-incubation with 1 μ M WMS-1410 completely prevented this effect. Glutamate, the physiological stimulus of the ionotropic NMDAR, AMPA and kainate receptors was also tested for any impact on islet cell viability. This series of experiments showed that the influence of glutamate was highly variable, ranging from no effect to a clear elevation of apoptotic cell death. Overall, the data showed no dose-response correlation (fraction of apoptotic cells after treatment with 0.5 mM glutamate 7 ± 4 %, $n=7$ vs. 5 mM glutamate: 9 ± 6 %, $n=6$) and did not culminate in statistically

significant cell death even after 7 days of culture (Fig. 1E, F). Consequently, we could not detect any beneficial effect of WMS-1410, but only a slight tendency with the higher concentration of 1 μ M.

WMS-1410 prevents the pro-apoptotic influence of glucolipotoxicity

Progressive loss of functional beta cells by elevated metabolic stress is a driving force fostering manifestation of type 2 diabetes mellitus. There are several models to mimic excessive nutrient supply *in vitro*. Lipotoxic conditions can be induced either by pharmacological stimulation of intracellular lipid synthesis or by providing a high extracellular lipid concentration. We used both methods, in combination with a supra-physiological glucose concentration to create a “glucolipotoxic” milieu. The LXR agonist T0901317 (10 μ M) was chosen to elevate lipid generation and palmitate (500 μ M) was applied to challenge the islet cells from the outside in medium supplemented with 33 mM glucose for a period of 7 days. Both models resulted in a clear rise in the fraction of apoptotic islet cells (Fig. 2A, B, grey vs. white bars). Co-culture with WMS-1410 (1 μ M) showed no effect in the LXR-glucolipotoxic model (Fig. 2A). By contrast, WMS-1410 was clearly protective in the palmitate-glucolipotoxic model. The effect amounted to ~30 % with 0.1 and ~60 % with 1 μ M of the GluN2B antagonist WMS-1410 (Fig. 2B). Ro 25-6981 (1 μ M), another inhibitor of GluN2B (Fischer et al., 1997) exerted a similar, beneficial effect (Fig. 2C). In line with this, the non-selective and low-affinity NMDAR blocker memantine (Bresink et al., 1996) also reduced the pro-apoptotic influence of glucolipotoxicity (Suppl. Fig. 1A). As the attenuation of glucolipotoxicity-induced cell death in single islet cells implicates improvement of insulin release, whole islets were cultured in the presence of high glucose and palmitate. In contrast to the hypothesis, co-culture with WMS-1410 (1 μ M) only resulted in a small, statistically non-significant rise in insulin secretion and thus was not able to preserve the secretory response (Fig. 2D). Determination of the insulin content revealed that glucolipotoxicity drastically reduced the insulin content independent of further treatment with WMS-1410 (Fig. 2E).

Analysis of insulin release as percentage of content showed that WMS-1410 increased the exocytotic process but, obviously, this was not sufficient to outweigh the severe effect of glucolipotoxicity on insulin biosynthesis (Fig. 2F).

Influence of NMDAR on membrane potential and intracellular Ca^{2+} concentration

As electrical activity and intracellular Ca^{2+} concentration ($[\text{Ca}^{2+}]_c$) play a central role for regulation of insulin secretion, the influence of NMDA on these parameters was investigated. Upon activation of NMDAR, Ca^{2+} influx through these ion channels should lead to a depolarization of the membrane potential and consequently open voltage-dependent Ca^{2+} channels (Inagaki et al., 1995). On the other hand, there is evidence that NMDAR activation finally triggers a negative feedback via Ca^{2+} -regulated K^+ channels and K_{ATP} channels (Marquard et al., 2015). To evaluate this, the pattern of oscillations of the electrical activity was investigated in islets cultured on microelectrode arrays. Stimulation of islets with 8 mM glucose resulted in regular oscillations. Calculation of the fraction of plateau phase (FOPP), i.e. the time where the membrane was depolarized, resulted in an average value of 12 %. Acute application of NMDA/glycine (500/10 μM) neither changed the FOPP nor prolonged the electrically silent interburst intervals (Fig. 3A). For a more detailed analysis, we performed patch-clamp experiments, in which the influence of NMDA on Ca^{2+} action potentials and absolute membrane potential was tested. In the perforated-patch configuration where cell metabolism is intact, typical Ca^{2+} action potentials were visible in the presence of 15 mM glucose. After this functional test for metabolic integrity glucose concentration was lowered to 5 or 4 mM to decrease the number of action potentials close to the threshold for stimulation of electrical activity. This maneuver creates conditions, where alterations in both directions could be detected. Thereafter, NMDA/glycine was added to the bath solution. Three out of nine beta cells reacted with an increase in Ca^{2+} action potentials (Fig. 3B), whereas six cells responded with a membrane potential hyperpolarization (Fig. 3C). To see how NMDA influenced $[\text{Ca}^{2+}]_c$ when the glucose concentration was lowered below the

threshold for Ca^{2+} oscillations, similar experiments were performed in cells loaded with the Ca^{2+} -sensitive fluorescence dye Fura-2. Beta cells responded with typical Ca^{2+} oscillations that disappeared when glucose was lowered from 15 to 5 mM. When NMDA/glycine (500/10 μM) was applied under these conditions, the maneuver was without any effect in 26 out of 34 β -cells and $[\text{Ca}^{2+}]_c$ remained low until glucose was elevated to 15 mM again (Fig. 4A, black trace in the exemplary recording). In 8 islet cells a Ca^{2+} rise or a Ca^{2+} peak could be detected in response to NMDA (Fig. 4A, grey trace). A succeeding set of experiments revealed that this effect of NMDA was prevented by WMS-1410 (1 μM) in 4 out of 9 cells reacting to NMDA in the washout phase (Fig. 4B).

As outlined before (Fig. 1A-D), WMS-1410 was highly effective in preventing the negative effects of prolonged exposure of the islet cells and islets, respectively, to NMDA with respect to cell viability and insulin release. Based on the observation that acute application of NMDA was able to elevate $[\text{Ca}^{2+}]_c$ in a subset of islet cells only, the influence of continuous receptor activation on $[\text{Ca}^{2+}]_c$ was investigated. Whole mouse islets were used for this series of experiments. To evoke typical Ca^{2+} oscillations the islets were treated with bath solution containing 15 mM glucose (Fig. 4C). The metabolic integrity of the islets was confirmed by switching the glucose concentration from 15 to 0.5 mM glucose at the end of each experiment. Mean Ca^{2+} (calculated over a period of 15 minutes) in response to 15 mM glucose did not differ between islets cultured with control medium and islets cultured in standard culture medium supplemented with NMDA (500 μM) for 24 hours. By contrast, the addition of WMS-1410 (1 μM) to the latter culture condition for 24 hours changed the pattern of oscillations in islets exposed to 15 mM glucose. Oscillations were faster and $[\text{Ca}^{2+}]_c$ did not return to a basal level between oscillations or remained in a long plateau phase after rising (Fig. 4C, lower vs. upper exemplary recording). Consequently, mean Ca^{2+} was higher in WMS-1410-preincubated islets (Fig. 4C, diagram). These data suggest that the protective effect of WMS-1410 on the NMDA-mediated lowering of insulin release (Fig. 1D) was achieved by two factors: preserved beta cell mass and an increased Ca^{2+} influx in response

to glucose stimulation. Control experiments were performed (Suppl. Fig. 1B) to exclude that WMS-1410 influences $[Ca^{2+}]_c$ by off-target effects on the K_{ATP} channel, which is the most important ion channel coupling glucose metabolism to $[Ca^{2+}]_c$.

NMDAR activation and GluN2B inhibition have no effect on insulin release under physiological conditions

The data presented above illustrated that NMDA had only small effects on membrane potential and $[Ca^{2+}]_c$ at threshold glucose concentrations and no effect on membrane potential oscillations or $[Ca^{2+}]_c$ at stimulatory glucose concentrations. These observations were reflected in the lack of any acute effect of NMDA (500 μ M, in combination with 10 μ M glycine) on insulin release (1-hour steady state incubation) at glucose concentrations of 6, 8, 10 and 15 mM (Fig. 5A). The combined application of WMS-1410 (1 μ M) and NMDA did not change this result (Fig. 5B).

Finally, the influence of WMS-1410 on islets not exposed to any pathological environment or NMDA was investigated. Isolated islets were treated with 1 μ M WMS-1410 for different periods of time (Fig. 5C). As expected, WMS-1410 did not change secretion, when added during the 1-hour steady state incubation with 15 mM glucose. Secretion was also unaffected when the islets were cultured for 7 days in standard medium supplemented with WMS-1410 (1 μ M) and thereafter acutely stimulated by 15 mM glucose for 1 hour.

Discussion

Beta cell signalling during acute vs. continuous NMDAR activation

The influence of NMDA and NMDAR activation on insulin secretion was investigated by several groups but the results are heterogeneous (Gonoi et al., 1994; Inagaki et al., 1995; Molnár et al., 1995; Marquard et al., 2015; Patterson et al., 2016; Huang et al., 2017a; Lockridge et al., 2021). The reasons are manifold including variations in time, concentration of NMDA or glucose, co-stimuli or differences in species. In our experiments, acute exposure of the islets to NMDA neither affected insulin release at the threshold for glucose-induced insulin release nor at stimulatory glucose concentrations (Fig. 5A). This lack of effect fits to the microarray data illustrating that the fraction of plateau phase was not altered by NMDA/glycine (Fig. 3A). NMDA also did not prolong the interburst intervals, an effect one would expect following the idea that - in addition to Ca^{2+} influx via the L-type Ca^{2+} channels - NMDARs interact with and contribute to the negative feedback loop regulating the oscillatory activity of pancreatic islets (Krippeit-Drews et al., 2000; Marquard et al., 2015). Our data suggest that either the NMDAR is not involved in this mechanism or that its contribution due to the irregular distribution (Patterson et al., 2016; Wu et al., 2017) is too small to be detected as a single regulatory component under these experimental conditions. At lower glucose concentrations, our investigation of membrane potential and $[\text{Ca}^{2+}]_c$ revealed subtle changes depending on the status of activity of the single cells. In beta cells that displayed Ca^{2+} action potentials at a low frequency, acute application of NMDA/glycine depolarized membrane potential and accelerated the action potentials. Wu *et al.* also described an initial depolarization in response to NMDA/glycine for a subset of human beta cells (Wu et al., 2017). By contrast, cells with a high action potential frequency at threshold glucose concentrations responded with a hyperpolarization (Fig. 3C). The latter observation might indicate an activation of K^+ channels (K_{ATP} and/or Ca^{2+} -activated channels) by the additional Ca^{2+} influx via NMDAR at an already existing, high level of $[\text{Ca}^{2+}]_c$. To see whether NMDA/glycine-induced effects at substimulatory glucose levels could be monitored by

determination of global $[Ca^{2+}]_c$, we performed experiments in which glucose was lowered slightly below the threshold for Ca^{2+} influx. Treatment with NMDA/glycine induced a Ca^{2+} peak or a sustained, small increase in 24 % of all cells (Fig. 4A). This is congruent to data of Inagaki et al., 1995 with rat islets showing an NMDA-induced rise in $[Ca^{2+}]_c$ in a low number (11 %) of all glucose-responsive islet cells. Currently it is not clear, why the fraction of NMDA-responsive cells is rather small. However, as only less than 50 % of cells contain the mandatory GluN1 subunit, less than half of the cells may express functional NMDAR as suggested for human beta cells and for insulin-secreting INS-832/13 cells (Wu et al., 2017). Treatment with the GluN2B selective compound WMS-1410 further reduced the number of NMDA-responsive islet cells to 15 % (Fig. 4B) indicating that NMDARs with this subunit are functionally active in islet cells.

Contrasting to the small alterations induced by acute activation of NMDAR, a prolonged, 24-hour incubation with NMDA reduced glucose-mediated insulin release by about 30 % (Fig. 1D). This effect was not correlated to any alteration in $[Ca^{2+}]_c$ (Fig. 4C). Our data indicate that the elevated rate of apoptosis might be the reason for the impairment of islet function. Up to now the mechanisms inducing apoptosis remain to be elucidated. It was suggested that mitochondrial damage by oxidative stress as well as induction of ER stress play a decisive role (Huang et al., 2019). In agreement with this, we observed a rise in the fluorescence of the ROS-sensitive dye DCF after long-term treatment with a high concentration of NMDA (Fig. 1A). The fact that the Ca^{2+} signaling of islets was not impaired after a 24-hour exposure to 500 μ M NMDA argues against a mechanism involving a dramatic decrease in mitochondrial ATP production. Accordingly, determination of the influence of NMDA on ATP content and the ATP to ADP ratio in the mouse insulinoma cell line MIN6 cells showed a decrease by 5 and 10 mM NMDA, while 1 mM NMDA was ineffective (Huang et al., 2017b).

Protective effects of WMS-1410 on murine pancreatic islets under stress conditions

Our data demonstrate for the first time that blocking NMDAR via GluN2B interacts with apoptotic beta cell death. In agreement with the detrimental role of oxidative stress as a trigger for apoptotic pathways (Drews et al., 2010), protection against NMDA-induced cell stress by WMS-1410 reduced the rise in cell death. As the beneficial effect of WMS-1410 on apoptosis was only partial, we tested whether this was enough to counteract the decline in insulin release in response to treatment with NMDA/glycine. Indeed, acute glucose-mediated insulin secretion reached the level of control when GluN2B-containing NMDARs were inhibited during the 24-hour culture of islets with NMDA/glycine (Fig. 1D). While several reports address the impact of NMDAR antagonists under physiological conditions, data with diabetic *in vivo* or *in vitro* models is scarce. Treatment of streptozotocin-diabetic mice with the NMDAR antagonist memantine attenuated the diabetic phenotype and lowered the rate of caspase3-positive islet cells (Huang et al., 2017a). In leptin receptor-deficient (db/db) mice, 3 mg/ml dextromethorphan in the drinking water ameliorated the time-dependent development of hyperglycemia compared to treatment with 1 mg/ml of the drug (Marquard et al., 2015). This was accompanied by a rise in insulin content. As we have previously shown that dextromethorphan exerts unspecific effects on L-type Ca^{2+} and K_{ATP} channels (Gresch & Düfer, 2020), the contribution of NMDAR inhibition to the observed effects remains unclear. As lipids considerably promote beta cell damage during development of type 2 diabetes mellitus (Lytrivi et al., 2020), we used two approaches to address the influence of GluN2B-selective inhibition of NMDAR on apoptosis in an environment mimicking the *in vivo* situation in an *in vitro* model. On the one hand, high glucose was combined with palmitate, on the other hand, the LXR activator T0901317 was used to interfere with intracellular lipid handling by fostering intracellular lipid accumulation (Choe et al., 2007). In the high glucose/palmitate model, WMS-1410 and Ro 25-6981 markedly reduced the rate of apoptosis (Fig. 2B and C). By contrast, the NMDAR inhibiting approach was not effective in the high glucose/T0901317 model (Fig. 2A). At a first glance, the latter result might appear contradictory, as T0901317 increases apoptotic cell death similar to the effect observed with palmitate in our experiments

with islet cells and was reported to decrease insulin secretion in MIN6 cells (Meng et al., 2012). Meanwhile, it is known that this compound directly inhibits mitochondrial respiration (Maczewsky et al., 2017) and exerts unspecific effects in islet cells of LXR α/β -double-knockout mice (Maczewsky et al., 2020). Consequently, it is not astonishing that inhibition of NMDAR via GluN2B could not prevent this rather unspecific cell damage rendering this model system unsuitable. The experiments with high glucose/palmitate demonstrate, that glucose-stimulated insulin release could not be rescued by WMS-1410 despite of a partial recovery of cell viability. Further investigations revealed that this lack of positive effect was due to a dramatic decline in insulin content that remained unaffected by the NMDAR subunit GluN2B inhibition. A reduction of insulin mRNA was reported for MIN6 and RINm5F cells in response to 33 mM glucose (Huang et al., 2017a). However, this effect could be counteracted by MK-801 or knockdown of the GluN1 subunit. The reason for this discrepancy might be based on several factors: First, the effect of high glucose without concomitant lipid challenge on insulin release and insulin expression was less pronounced compared to our glucolipotoxic model. Lipids substantially contribute to the impairment of beta cell function during progression of type 2 diabetes mellitus (Zhou & Grill, 1995; Poirout et al., 2010) and a dual hit by both nutrients in excess seem to be too harmful to be outweighed by targeting NMDAR. Second, MK-801 or knockdown of GluN1 affects all subtypes of NMDAR and not only those, composed of GluN2B. As various NMDAR subunits have been shown to be present in pancreatic islets or insulin secreting cell lines (Gonoi et al., 1994; Inagaki et al., 1995; Morley et al., 2000; Patterson et al., 2016; Cochrane et al., 2020), our data are in line with the expectation that the GluN2B subunit is not part of all NMDA-gated ion channels. Finally, as only approximately half of the beta cells express detectable amounts of GluN1, not all glucolipotoxicity-induced damages are accessible to NMDAR modulation (Wu et al., 2017). Interestingly, we observed an increase in $[Ca^{2+}]_c$ when the islets were treated with NMDA in combination with WMS-1410 for 24 h. This indicates activation of a compensatory mechanism and might be the reason for the slight trend to an increased

secretory response but, obviously, elevated Ca^{2+} influx is not enough to protect cell function against the manifold effects of glucolipotoxicity.

In summary, this study shows that acute activation of NMDAR does not severely interact with the stimulus-secretion coupling whereas excessive stimulation of the receptor leads to oxidative stress, fosters cell death, and decreases insulin release. Targeting the GluN2B subunit of NMDAR protects against oxidative stress and decreases the rate of apoptotic cell death observed in the NMDA model and in an *in vitro* glucolipotoxicity model (Fig. 6B). Further studies with *in vivo* approaches are necessary to evaluate whether modulators of the GluN2B isoform are suited to support the maintenance of glycemic control in type 2 diabetes mellitus.

Acknowledgement

We thank Melanie Arning and Katrin von Schroetter for skillful technical assistance.

Author contributions

Participated in research design: Gresch, Düfer

Conducted experiments: Gresch, Noguera Hurtado, Wiggers, Wörmeyer, De Luca

Contributed new reagents or analytic tools: Wunsch

Performed data analysis: Gresch, Noguera Hurtado, Wörmeyer, Wiggers, Rübiger

Wrote or contributed to the writing of the manuscript: Düfer, Gresch, Wunsch, Seebohm

References

- Arntfield ME & van der Kooy D** (2011) β -Cell evolution: How the pancreas borrowed from the brain: The shared toolbox of genes expressed by neural and pancreatic endocrine cells may reflect their evolutionary relationship. *Bioessays* 33 (8):582–587.
- Atouf F, Czernichow P, and Scharfmann R** (1997) Expression of neuronal traits in pancreatic beta cells. Implication of neuron-restrictive silencing factor/repressor element silencing transcription factor, a neuron-restrictive silencer. *J Biol Chem* 272 (3):1929–1934.
- Bresink I, Benke TA, Collett VJ, Seal AJ, Parsons CG, Henley JM, and Collingridge GL** (1996) Effects of memantine on recombinant rat NMDA receptors expressed in HEK 293 cells. *Br J Pharmacol* 119 (2):195–204.
- Chazot PL** (2004) The NMDA receptor NR2B subunit: a valid therapeutic target for multiple CNS pathologies. *Curr Med Chem* 11 :389–396.
- Choe SS, Choi AH, Lee J-W, Kim KH, Chung J-J, Park J, Lee K-M, Park K-G, Lee I-K, and Kim JB** (2007) Chronic activation of liver X receptor induces beta-cell apoptosis through hyperactivation of lipogenesis: liver X receptor-mediated lipotoxicity in pancreatic beta-cells. *Diabetes* 56 (6):1534–1543.
- Cochrane VA, Wu Y, Yang Z, ElSheikh A, Dunford J, Kievit P, Fortin DA, and Shyng S-L** (2020) Leptin modulates pancreatic β -cell membrane potential through Src kinase-mediated phosphorylation of NMDA receptors. *J Biol Chem* 295 (50):17281–17297.
- Drews G, Krippeit-Drews P, and Düfer M** (2010) Oxidative stress and beta-cell dysfunction. *Pflugers Arch* 460 (4):703–718.
- Fischer G, Mutel V, Trube G, Malherbe P, Kew JN, Mohacsi E, Heitz MP, and Kemp JA** (1997) Ro 25-6981, a highly potent and selective blocker of N-methyl-D-aspartate receptors containing the NR2B subunit. Characterization in vitro. *J Pharmacol Exp Ther* 283 (3):1285–1292.

Gonoi T, Mizuno N, Inagaki N, Kuromi H, Seino Y, Miyazaki J, and Seino S (1994)

Functional neuronal ionotropic glutamate receptors are expressed in the non-neuronal cell line MIN6. *J Biol Chem* 269 (25):16989–16992.

Grapengiesser E, Gylfe E, and Hellman B (1988) Glucose-induced oscillations of

cytoplasmic Ca^{2+} in the pancreatic β -cell. *Biochem Biophys Res Commun* 151 (3):1299–1304.

Gresch A & Düfer M (2020) Dextromethorphan and dextrorphan influence insulin secretion

by interacting with K_{ATP} and L-type Ca^{2+} channels in pancreatic β -Cells. *J Pharmacol Exp Ther* 375 (1):10–20.

Huang X-T, Li C, Peng X-P, Guo J, Yue S-J, Liu W, Zhao F-Y, Han J-Z, Huang Y-H,

Yang-Li, **Cheng Q-M, Zhou Z-G, Chen C, Feng D-D, and Luo Z-Q (2017a)** An excessive increase in glutamate contributes to glucose-toxicity in β -cells via activation of pancreatic NMDA receptors in rodent diabetes. *Sci Rep* 7 :44120.

Huang X-T, Liu W, Zhou Y, Sun M, Sun C-C, Zhang C-Y, and Tang S-Y (2019)

Endoplasmic reticulum stress contributes to NMDA-induced pancreatic β -cell dysfunction in a CHOP-dependent manner. *Life Sci* 232 :116612.

Huang X-T, Yue S-J, Li C, Huang Y-H, Cheng Q-M, Li X-H, Hao C-X, Wang L-Z, Xu J-P,

Ji M, Chen C, Feng D-D, and Luo Z-Q (2017b) A sustained activation of pancreatic NMDARs is a novel factor of β -cell apoptosis and dysfunction. *Endocrinology* 158 (11):3900–3913.

Inagaki N, Kuromi H, Gonoi T, Okamoto Y, Ishida H, Seino Y, Kaneko T, Iwanaga T,

and Seino S (1995) Expression and role of ionotropic glutamate receptors in pancreatic islet cells. *FASEB J* 9 (8):686–691.

Krippeit-Drews P, Düfer M, and Drews G (2000) Parallel oscillations of intracellular

calcium activity and mitochondrial membrane potential in mouse pancreatic β -cell. *Biochem Biophys Res Commun* 267 (1):179–183.

- Lockridge A, Gustafson E, Wong A, Miller RF, and Alejandro EU** (2021) Acute D-serine co-agonism of β -Cell NMDA receptors potentiates glucose-stimulated insulin secretion and excitatory β -cell membrane activity. *Cells* 10 (1).
- Lytrivi M, Castell A-L, Poitout V, and Cnop M** (2020) Recent insights into mechanisms of β -cell lipo- and glucolipotoxicity in type 2 diabetes. *J Mol Biol* 432 (5):1514–1534.
- Maczewsky J, Kaiser J, Krippeit-Drews P, and Drews G** (2020) Approved LXR agonists exert unspecific effects on pancreatic β -cell function. *Endocrine* 68 (3):526–535.
- Maczewsky J, Sikimic J, Bauer C, Krippeit-Drews P, Wolke C, Lendeckel U, Barthlen W, and Drews G** (2017) The LXR ligand T0901317 acutely inhibits insulin secretion by affecting mitochondrial metabolism. *Endocrinology* 158 (7):2145–2154.
- Marquard J, Otter S, Welters A, Stirban A, Fischer A, Eglinger J, Herebian D, Kletke O, Klemen MS, Stožer A, Wnendt S, Piemonti L, Köhler M, Ferrer J, Thorens B, Schliess F, Rupnik MS, Heise T, Berggren P-O, Klöcker N, Meissner T, Mayatepek E, Eberhard D, Kragl M, and Lammert E** (2015) Characterization of pancreatic NMDA receptors as possible drug targets for diabetes treatment. *Nat Med* 21 (4):363–372.
- Meng ZX, Yin Y, Lv JH, Sha M, Lin Y, Gao L, Zhu YX, Sun YJ, and Han X** (2012) Aberrant activation of liver X receptors impairs pancreatic beta cell function through upregulation of sterol regulatory element-binding protein 1c in mouse islets and rodent cell lines. *Diabetologia* 55 (6):1733–1744.
- Molnár E, Váradi A, McIlhinney RJ, and Ashcroft SJ** (1995) Identification of functional ionotropic glutamate receptor proteins in pancreatic β -cells and in islets of Langerhans. *FEBS Letters* 371 (3):253–257.
- Mony L, Kew JNC, Gunthorpe MJ, and Paoletti P** (2009) Allosteric modulators of NR2B-containing NMDA receptors: molecular mechanisms and therapeutic potential. *Br J Pharmacol* 157 (8):1301–1317.

Morley P, MacLean S, Gendron TF, Small DL, Tremblay R, Durkin JP, and Mealing G

(2000) Pharmacological and molecular characterization of glutamate receptors in the MIN6 pancreatic beta-cell line. *Neurol Res* 22 (4):379–385.

Paoletti P, Bellone C, and Zhou Q (2013) NMDA receptor subunit diversity: impact on receptor properties, synaptic plasticity and disease. *Nat Rev Neurosci* 14 (6):383–400.

Patterson S, Irwin N, Guo-Parke H, Moffett RC, Scullion SM, Flatt PR, and

McClenaghan NH (2016) Evaluation of the role of N-methyl-D-aspartate (NMDA) receptors in insulin secreting beta-cells. *Eur J Pharmacol* 771 :107–113.

Poitout V, Amyot J, Semache M, Zarrouki B, Hagman D, and Fontés G (2010)

Glucolipotoxicity of the pancreatic beta cell. *Biochim Biophys Acta* 1801 (3):289–298.

Schultheis J, Beckmann D, Mulac D, Müller L, Esselen M, and Düfer M (2019) Nrf2

activation protects mouse beta cells from glucolipotoxicity by restoring mitochondrial function and physiological redox balance. *Oxid Med Cell Longev* 2019 :7518510.

Takahashi H, Yokoi N, and Seino S (2019) Glutamate as intracellular and extracellular signals in pancreatic islet functions. *Proc Jpn Acad Ser B Phys Biol Sci* 95 (6):246–260.

Tewes B, Frehland B, Schepmann D, Schmidtke K-U, Winckler T, and Wünsch B

(2010a) Conformationally constrained NR2B selective NMDA receptor antagonists derived from ifenprodil: Synthesis and biological evaluation of tetrahydro-3-benzazepine-1,7-diols. *Bioorg Med Chem* 18 (22):8005–8015.

Tewes B, Frehland B, Schepmann D, Schmidtke K-U, Winckler T, and Wünsch B

(2010b) Design, synthesis, and biological evaluation of 3-benzazepin-1-ols as NR2B-selective NMDA receptor antagonists. *ChemMedChem* 5 (5):687–695.

Williams K (1993) Ifenprodil discriminates subtypes of the N-methyl-D-aspartate receptor: selectivity and mechanisms at recombinant heteromeric receptors. *Mol Pharmacol* 44 (4):851–859.

- Wu Y, Fortin DA, Cochrane VA, Chen P-C, and Shyng S-L** (2017) NMDA receptors mediate leptin signaling and regulate potassium channel trafficking in pancreatic β -cells. *J Biol Chem* 292 (37):15512–15524.
- Zhang X-M & Luo J-H** (2013) GluN2A versus GluN2B: twins, but quite different. *Neurosci Bull* 29 (6):761–772.
- Zhou YP & Grill V** (1995) Long term exposure to fatty acids and ketones inhibits B-cell functions in human pancreatic islets of Langerhans. *J Clin Endocrinol Metab* 80 (5):1584–1590.

Footnotes

This work was supported by the Deutsche Forschungsgemeinschaft (Research Training Group GRK 2515, Chemical Biology of Ion Channels). The authors have no conflict of interests to declare.

Legends for Figures

Figure 1: Targeting the GluN2B subunit of NMDAR reverses the effects of NMDA on DCF fluorescence, apoptosis, and insulin release. (A) Mouse islet cells cultured in standard medium (containing glycine) supplemented with 5 mM NMDA for 48 hours showed a rise in DCF fluorescence indicative of oxidative stress. WMS-1410 (1 μ M) protected against this effect. (B) Addition of NMDA (500 μ M) and glycine (10 μ M) to the buffer solution (KRH) induced a rise in apoptotic cell death that was partly reversed by co-application of 1 μ M WMS-1410 (18 hours). (C) Similar effects were observed with 0.1 μ M of the test compound. (D) Insulin release stimulated by 15 mM glucose (1 hour steady-state incubation) was decreased after 24-hour treatment of islets with NMDA (500 μ M) in standard medium. The effect was prevented by 1 μ M WMS-1410. (E, F) Addition of glutamate (E: 0.5, F: 5 mM) to the culture medium for 7 days tended to elevate apoptosis independent of the presence or absence of WMS-1410 (1 μ M). The number of independent mouse preparations (islet cells: A-C, E and F, islets: D) is indicated below the bars. Circles indicate female, triangles male mice. * $p \leq 0.05$, *** $p \leq 0.001$ as indicated by the bars and in (D) vs. all other conditions.

Figure 2: WMS-1410 protects against apoptosis induced by glucolipotoxicity but not against the decline in insulin content. 33 mM glucose were combined with either 10 μ M of the LXR agonist T0901317 (A) or 500 μ M BSA-bound palmitate (B-F) for 7 days to create a high-glucose/high lipid environment. (A) After a culture period of 7 days, apoptotic cell death increased in the G33/T0901317-model independent of co-culture with WMS-1410 (1 μ M). (B) By contrast, WMS-1410 (0.1 and 1 μ M) displayed a dose-dependent protective effect in the G33/palmitate-model. (C) Ro 25-6981 (1 μ M) also protected against G33/palmitate toxicity. (D) Insulin release in response to 15 mM glucose (1 hour) was lowered after 7-day culture in the presence of G33/palmitate. This effect was not prevented by WMS-1410 (1 μ M). (E, F) The decline in insulin secretion was paralleled by a marked decrease in insulin content (E), whereas the %-secretion (F) was unaffected by glucolipotoxic treatment and

even tends to rise when islets were acutely stimulated with 15 mM glucose after culture in the presence of WMS-1410 (1 μ M). The number of independent mouse preparations (circles: female, triangles: male mice) of islet cells (A-C) or islets (D-F) is indicated below the bars. *** $p \leq 0.001$ in (D) vs. all other conditions, in (E) vs. control with 3 and 15 mM glucose, ** $p \leq 0.01$ in (A) vs. all other conditions, * $p \leq 0.05$, #### $p \leq 0.001$ vs. GLT conditions, ## $p \leq 0.01$ vs. control, # $p \leq 0.05$ vs. control.

Figure 3: Influence of NMDA on electrical activity of islets and beta cells. (A) Acute application of NMDA/Glycine (500 μ M/Gly 10 μ M) to whole islets cultured on microelectrode arrays did not change the fraction of electrical activity (FOPP) of islets stimulated by 8 mM glucose. An exemplary recording is shown on the left, the diagrams summarize the FOPP and the averaged interburst intervals of all experiments. (B, C) At a glucose concentration around the threshold for activation (4-5 mM) cells with a low frequency of action potentials (B) were depolarized by NMDA/glycine (500 μ M/10 μ M). By contrast, NMDA/glycine abrogated action potentials in those cells displaying higher frequency of action potentials (C). The diagram summarizes the changes in membrane potential in those cells that were hyperpolarized (six out of nine) by NMDA/glycine. The number of experiments with islets (A) of 3 different preparations (females) or islet cells of 6 preparations (B and C: female (circles)/ male (triangles): 4/2) is indicated in the diagrams. * $p \leq 0.05$

Figure 4: Effects of NMDA and WMS-1410 on $[Ca^{2+}]_c$ of islet cells and islets. (A) Islet cells were stimulated with 15 mM glucose to test for metabolic integrity. Thereafter the glucose concentration was lowered until the oscillations stopped. Acute treatment with 500 μ M NMDA (+ 10 μ M glycine) induced a rise or a Ca^{2+} peak in 24 % of all cells tested. (B) When WMS-1410 (1 μ M) was added prior to the NMDA stimulus, the NMDA-induced rise in $[Ca^{2+}]_c$ was lowered to 15 %. Exemplary recordings are presented on the left of (A) and (B). Data are summarized in the pie charts. (C) 24-hour culture of islets in standard culture medium in

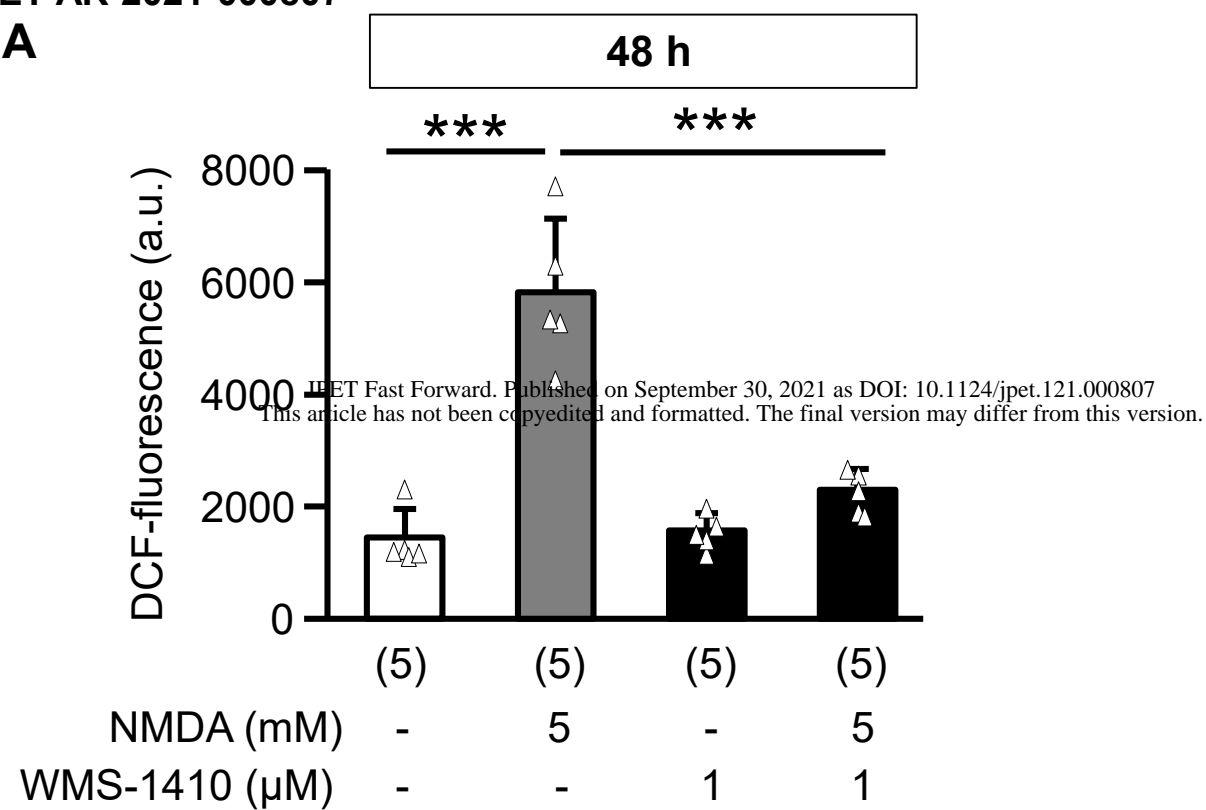
the presence or absence of NMDA (500 μ M) did not influence the oscillations in $[Ca^{2+}]_c$ evoked by 15 mM glucose (upper trace, dashed vs. continuous line). By contrast, $[Ca^{2+}]_c$ was proportionally shifted to a plateau when the islets were stimulated by 15 mM glucose after 24-hour treatment with WMS-1410 (1 μ M) in standard culture medium. Data are summarized in the diagram. The number of experiments with islet cells (A and B) or islets (C) refers to 3 independent preparations (A, B: females, C: female/male: 1/2). * $p \leq 0.05$ vs. all other conditions

Figure 5: NMDA or WMS-1410 have no effect on insulin release under physiological conditions. (A, B) Islets were incubated with different glucose concentrations in the presence or absence of (A) NMDA (500 μ M) and glycine (10 μ M) or (B) in combination with WMS-1410 (1 μ M) for 1 hour. (C) The effect of WMS-1410 (1 μ M) without NMDAR activation was tested acutely during the 1-hour secretion experiment and after culture in standard medium for 7 days. The numbers below the bars indicate the number of independent islet preparations (circles: female, triangles: male mice) *** $p \leq 0.001$ vs. all other conditions, ** $p \leq 0.01$ in (A) vs. 8 mM glucose \pm NMDA, in (B) vs. all other conditions, * $p \leq 0.05$ vs. 8 mM glucose \pm NMDA, ### $p \leq 0.001$ vs. 10 and 15 mM glucose \pm NMDA, §§ $p \leq 0.01$ vs. 15 mM glucose \pm NMDA. Please note that, for clearness of presentation, only the most relevant significances are included in (A).

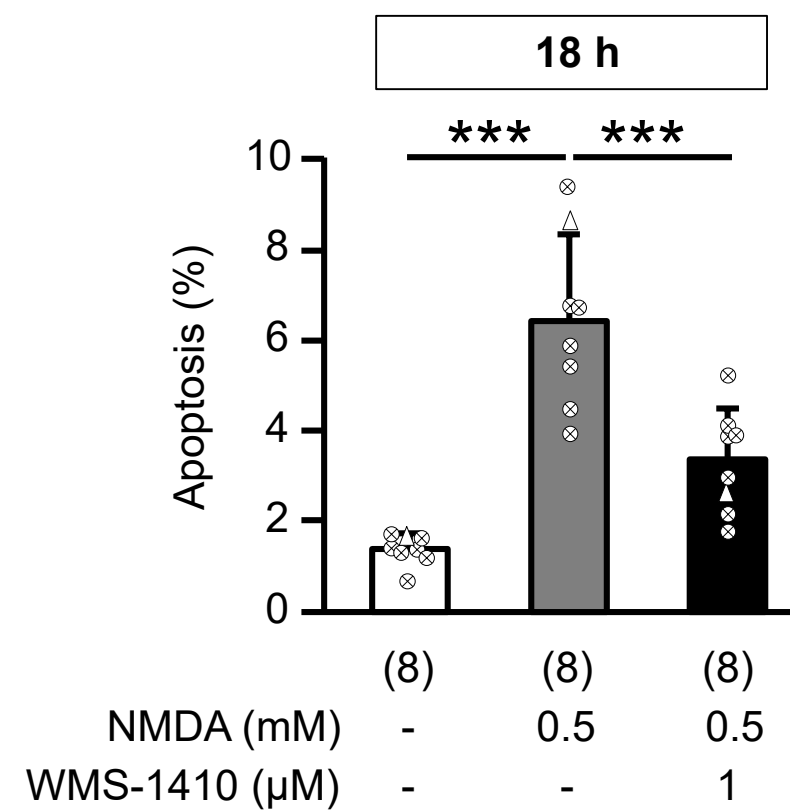
Figure 6: Summary of the influence of targeting NMDAR in pancreatic islets. (A) Structures of GluN2B-selective inhibitors WMS-1410 (a) and Ro 25-6981 (b). (B) Long-term (18 to 48 hours) application of NMDA on whole islets (illustrated by red arrows) lead to an increase in ROS and apoptosis. This decreases glucose-stimulated insulin release (GSIS) without impairment of Ca^{2+} oscillations. Acute treatment with NMDA (black arrows) does not alter GSIS. Of note, the mixed effects of NMDA on membrane potential and $[Ca^{2+}]_c$ in single beta cells (left) are not strong enough to affect the synchronized oscillations in whole islets (right).

Grey stars denote protection against NMDA-induced changes (ROS, apoptosis, GSIS) and modulation ($[Ca^{2+}]_c$) by WMS-1410. The black star points out that protection against apoptosis also occurs under glucolipotoxic conditions.

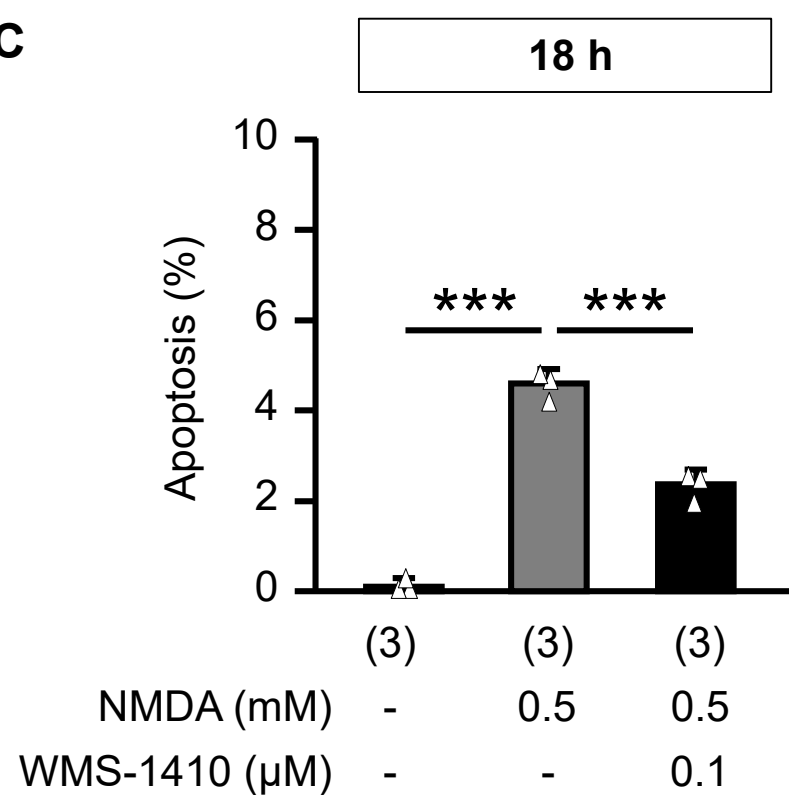
A



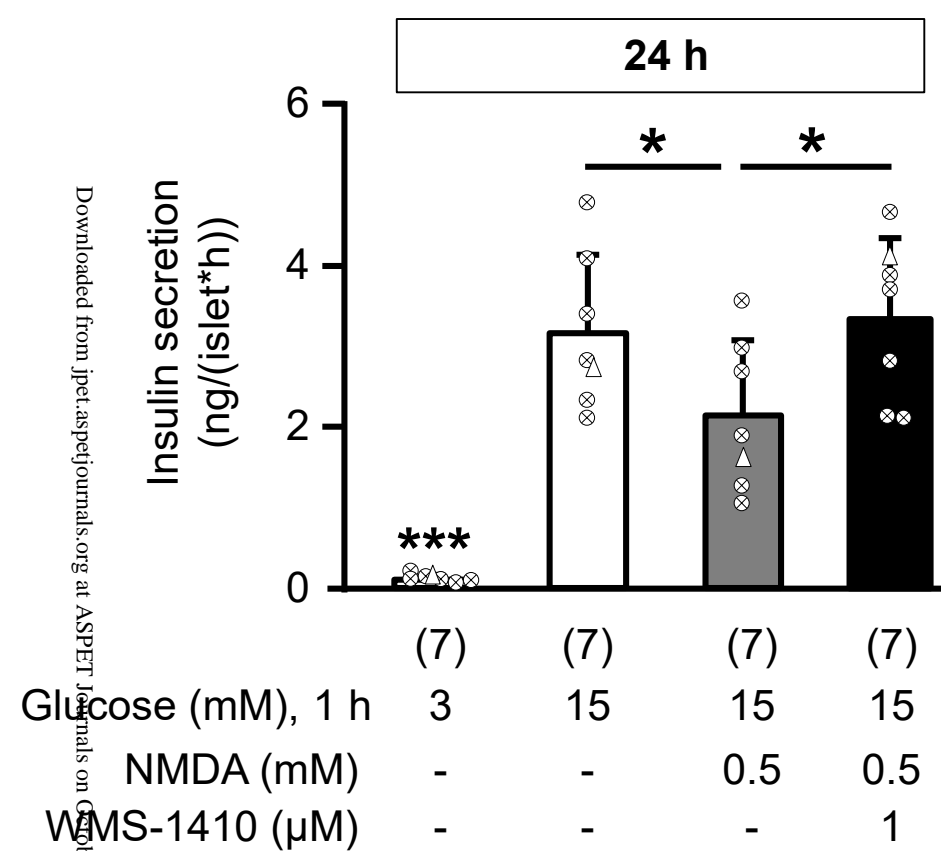
B



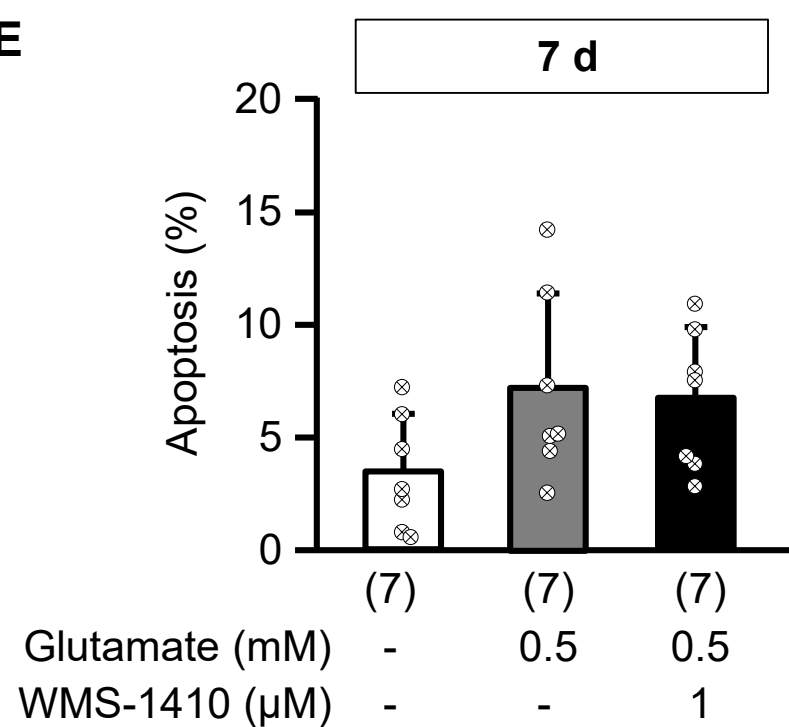
C



D



E



F

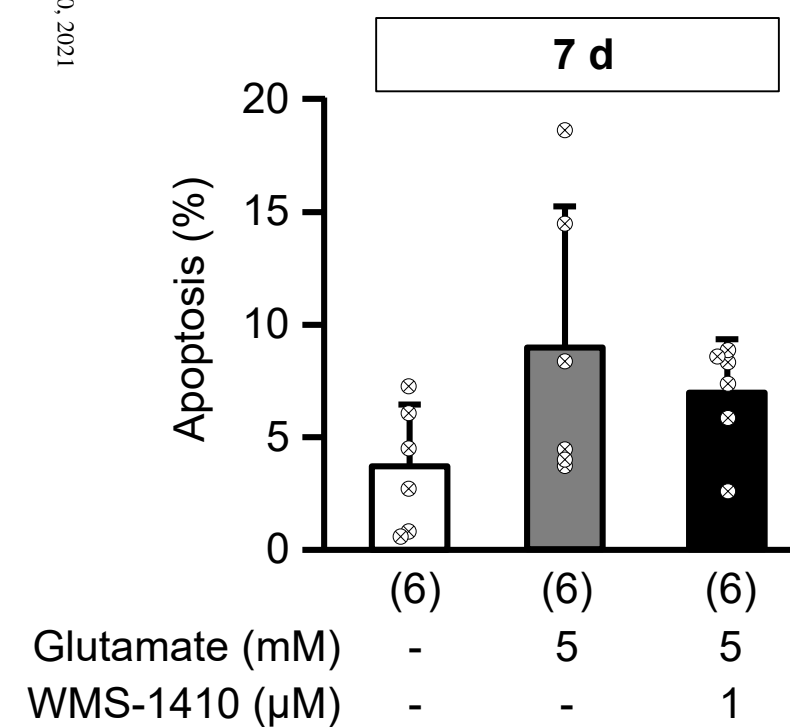


Figure 1

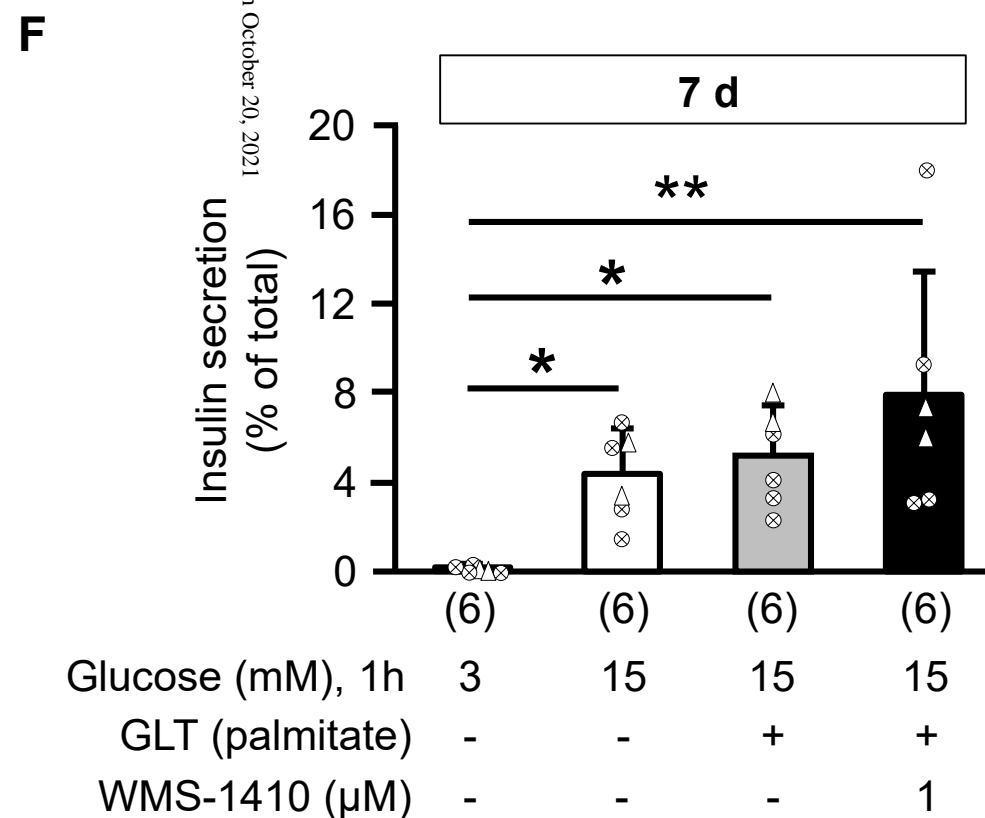
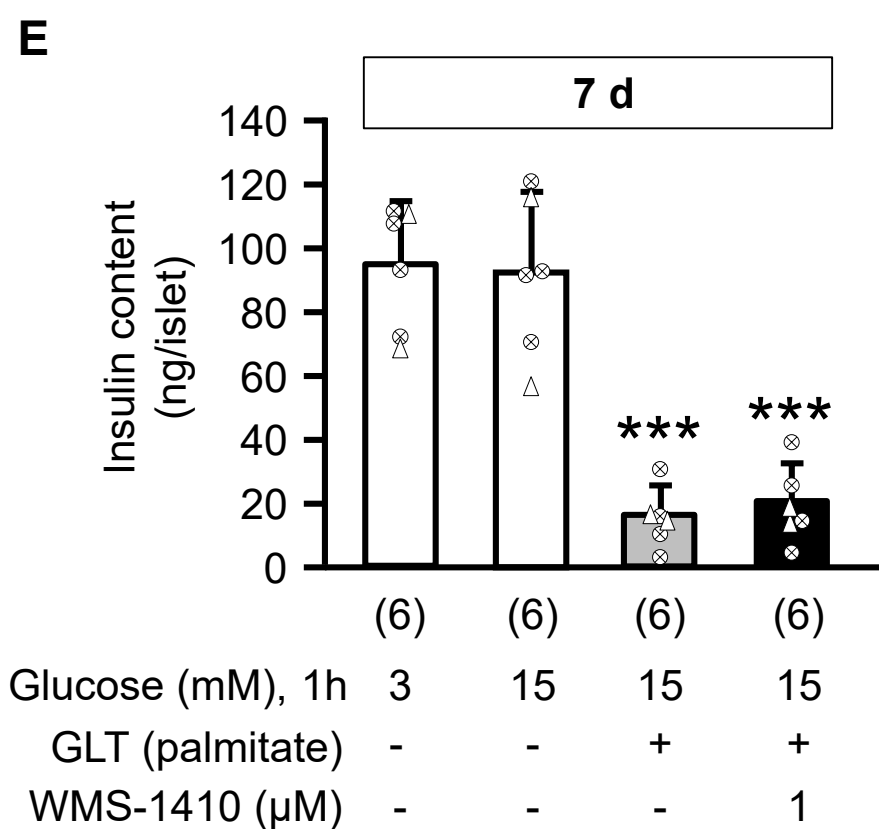
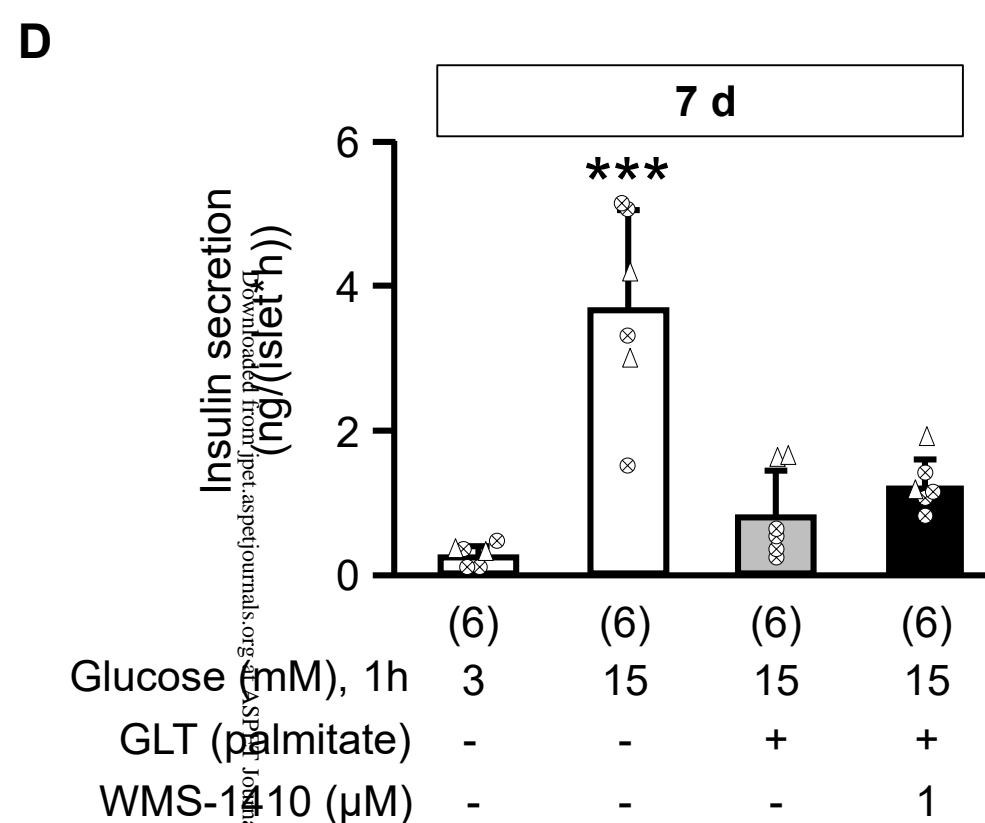
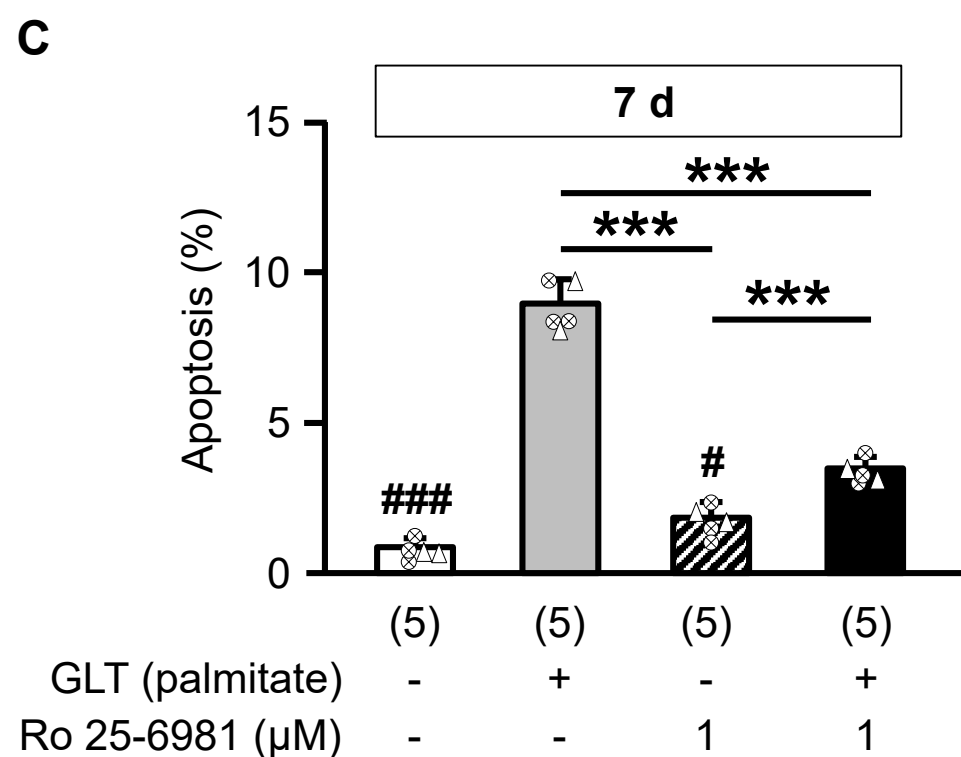
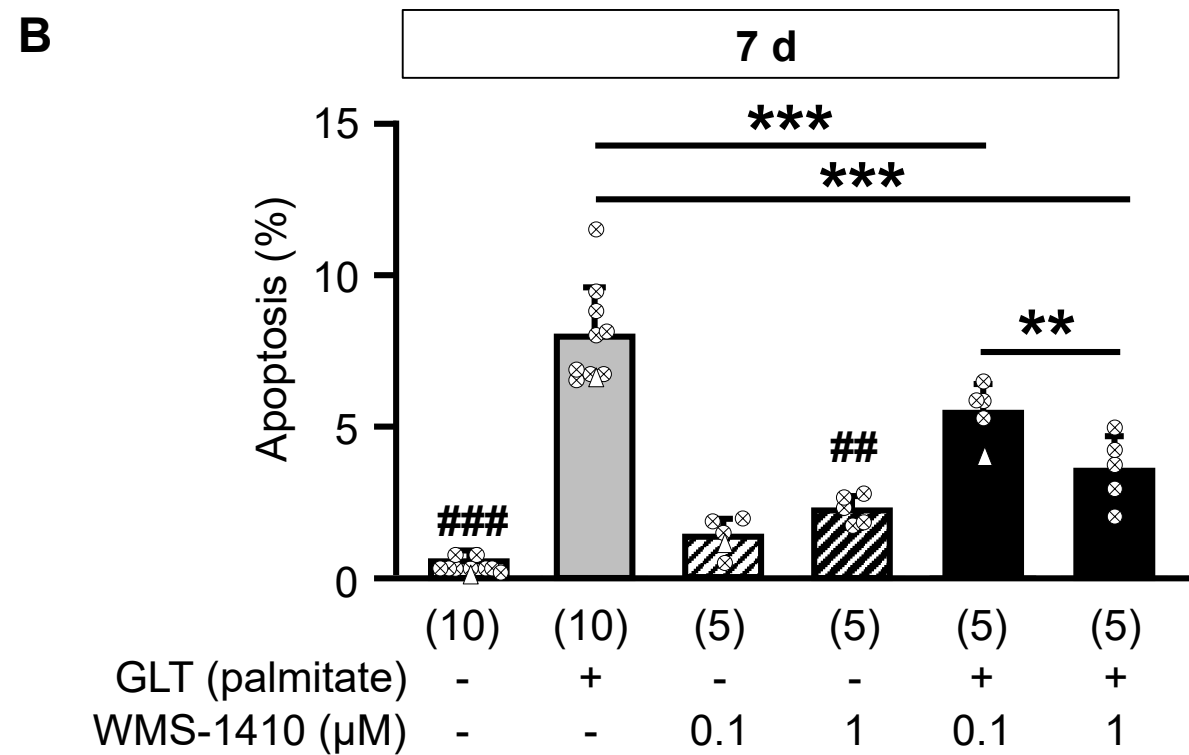
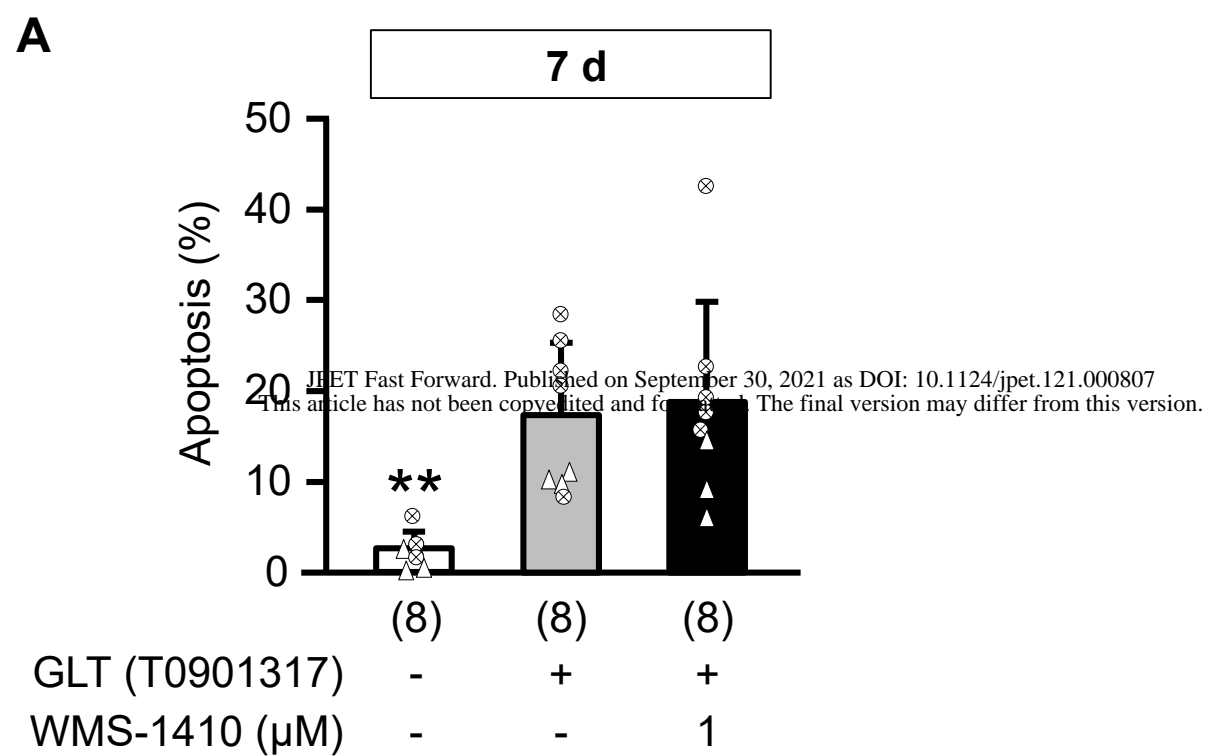
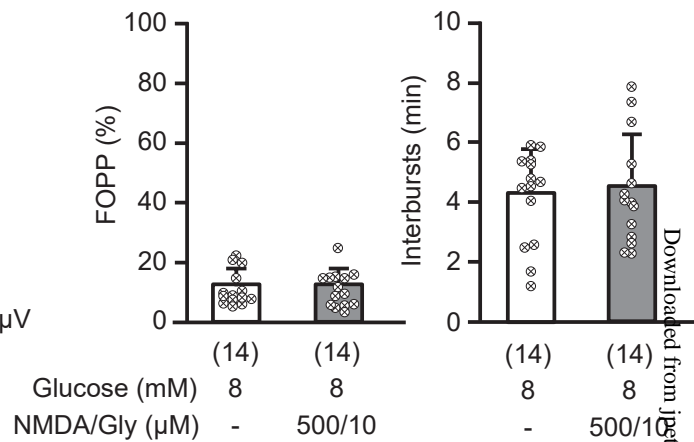
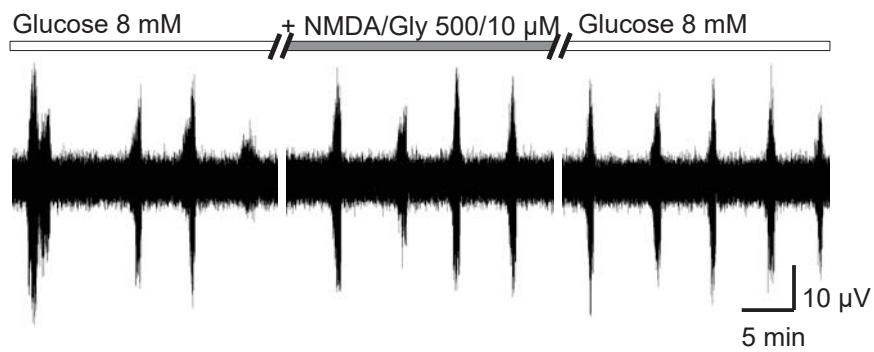
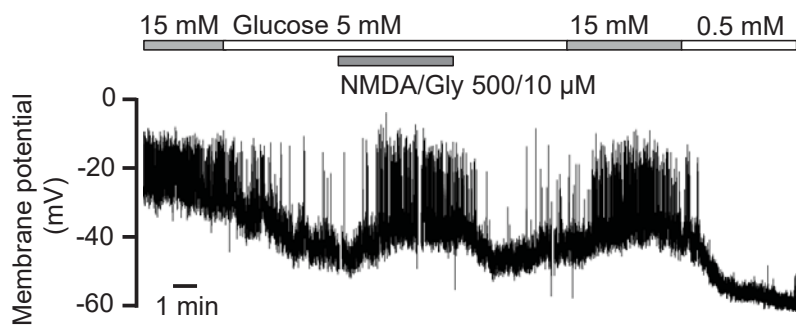


Figure 2

A



B



C

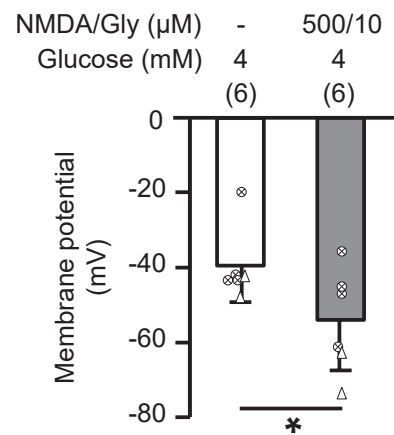
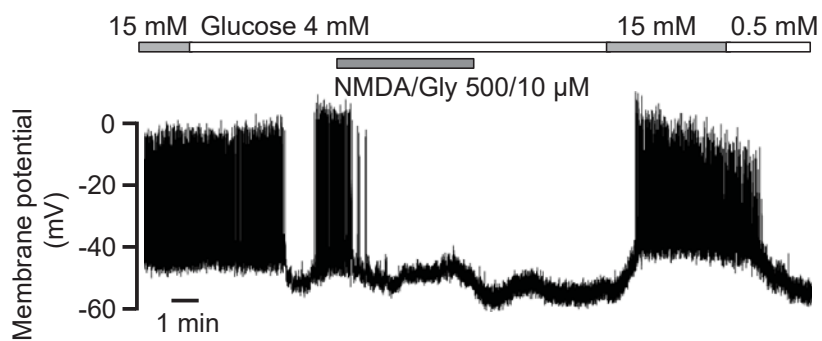


Figure 3

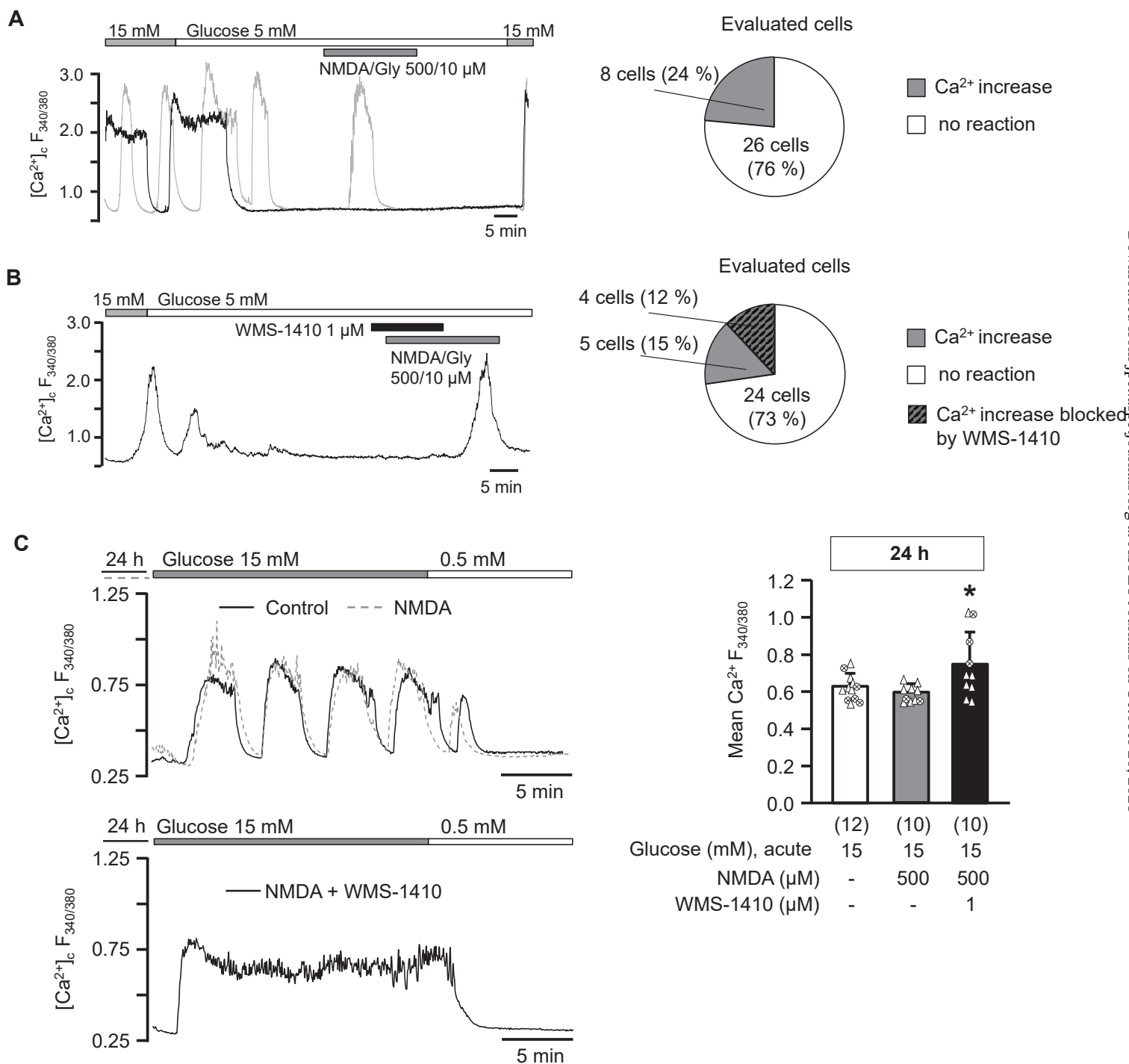


Figure 4

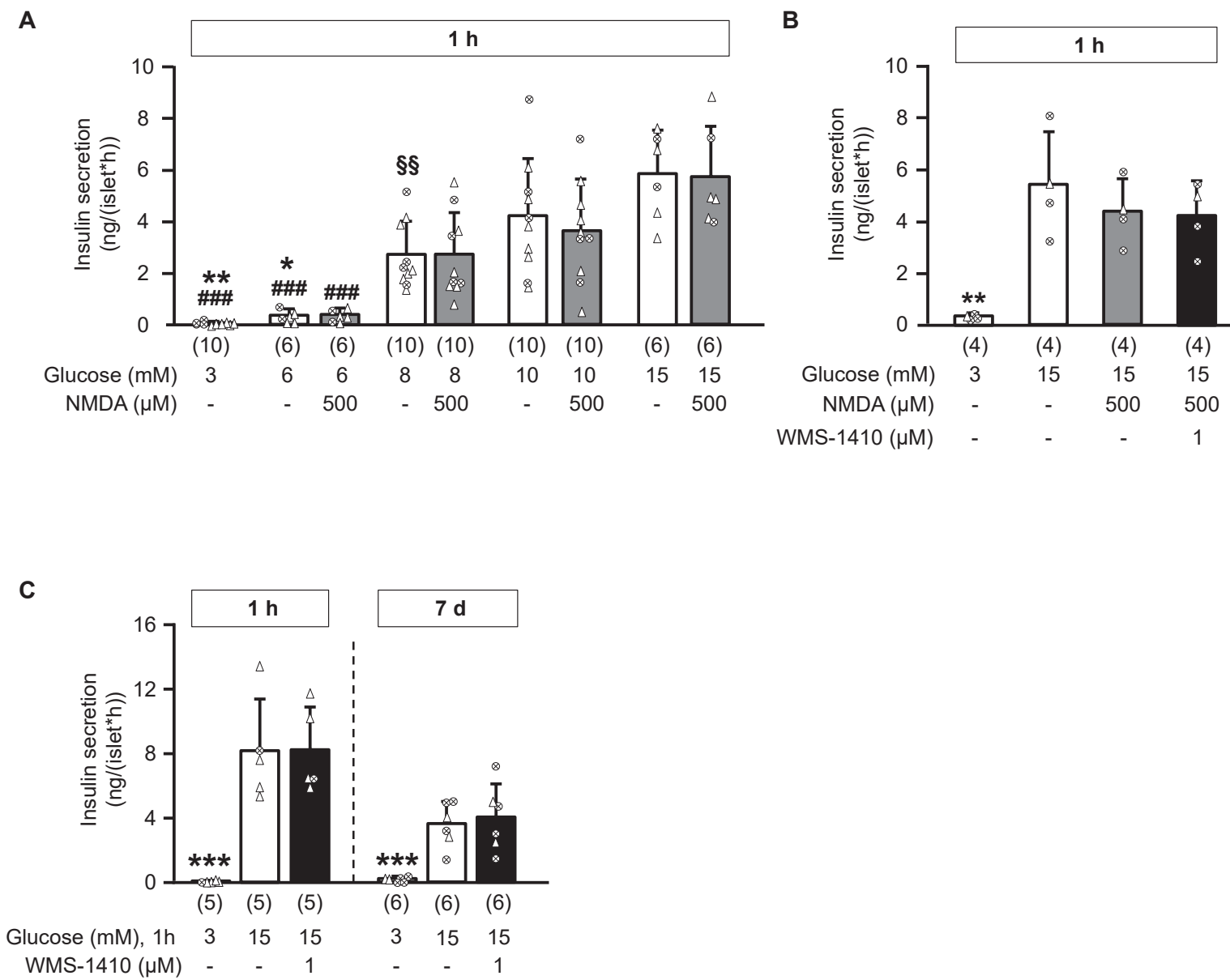
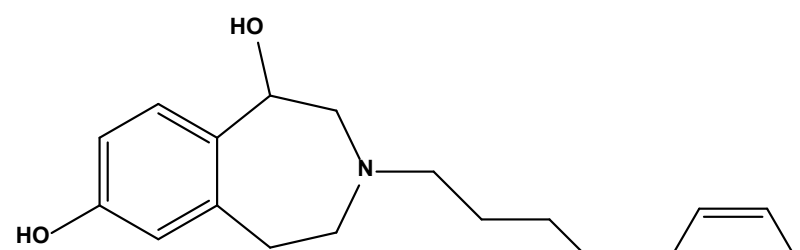


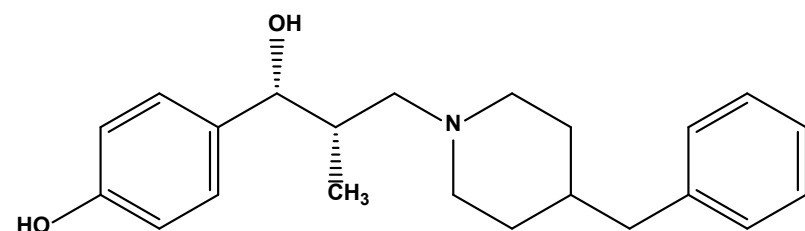
Figure 5

A



JPET Fast Forward. Published on September 30, 2021 as DOI: 10.1124/jpet.121.000807
This article has not been copyedited and formatted. The final version may differ from this version.

(a)



(b)

B

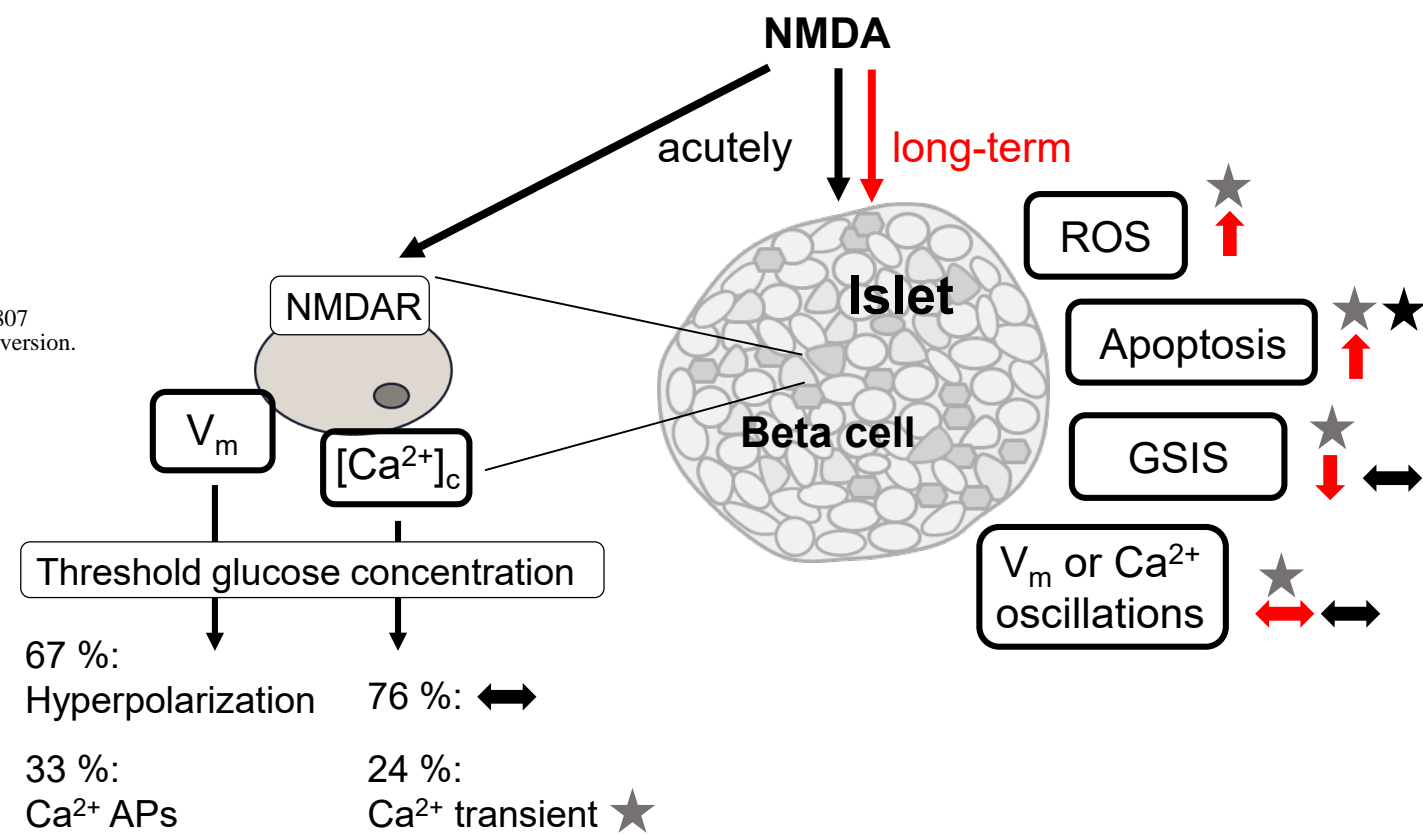


Figure 6

Supplementary Figure

Selective Inhibition of NMDA receptors with GluN2B subunit protects beta cells against stress-induced apoptotic cell death

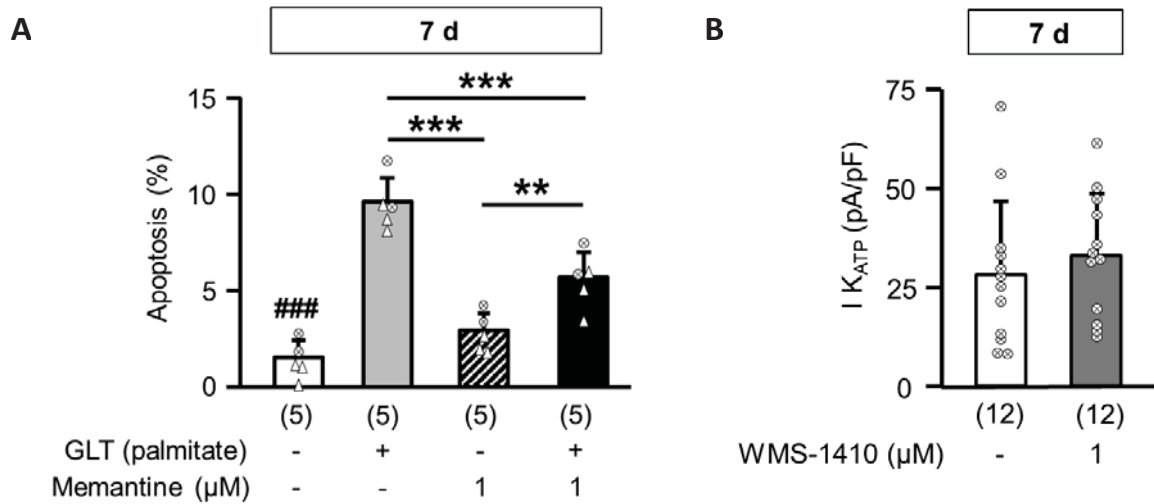
Anne Gresch^{a§}, Héctor Noguera Hurtado^{a§}, Laura Wörmeyer^a, Vivien De Luca^a, Rebekka Wiggers^a, Guiscard Seeböhm^b, Bernhard Wunsch^c, Martina Düfer^a

^a Pharmaceutical and Medicinal Chemistry, Dept. of Pharmacology, PharmaCampus, University of Münster, Corrensstraße 48, 48149 Münster, Germany

^b Institute for Genetics of Heart Diseases (IfGH), Department of Cardiovascular Medicine, University Hospital Münster, D-48149 Münster, Germany.

^c Pharmaceutical and Medicinal Chemistry, PharmaCampus, University of Münster, Corrensstraße 48, 48149 Münster, Germany

Supplementary Figure 1



Influence of memantine on glucolipotoxicity-induced apoptosis and effect of WMS-1410 on K_{ATP} current. (A) After a culture period of 7 days, apoptotic islet cell death increased in the G33/palmitate-model. The non-subunit-selective NMDAR blocker memantine (1 μM) partially protected against this. (B) K_{ATP} current of single beta cells was measured in the standard whole-cell configuration after 7 days of incubation with control medium \pm WMS-1410 (1 μM). The GluN2B-specific inhibitor did not affect the current. Recordings were performed with bath solution (0,5 mM glucose, see methods section of the main document). Pipette solution contained (in mM): 130 KCl, 4 MgCl_2 , 2 CaCl_2 , 10 EGTA, 0.65 Na_2ATP , 20 HEPES (pH 7.15). K_{ATP} current was recorded by application of 300-ms pulses to -60 mV and -80 mV, respectively, from a holding potential of -70 mV. The amplitude at -60 mV was evaluated (mean of 3 consecutive data points) when steady state was reached. At the end of each recording tolbutamide (100 μM) was added to verify the measurement of K_{ATP} currents. *** $p \leq 0.001$, ** $p \leq 0.01$, ### $p \leq 0.001$ vs. GLT conditions.